

FOULING THICKNESS MODELING FOR REFINERY CLEANING SCHEDULE OPTIMIZATION

*M. J. Bagajewicz^{1,2,3}, A. L. M. Nahes⁴ and A. L. H. Costa⁴

¹ OK-Solutions, Norman OK, USA (corresponding author)

² Refined Technologies, Houston, TX, USA

³ Federal University of Rio de Janeiro, Rio de Janeiro, Brazil.

⁴ State University of Rio de Janeiro, Rio de Janeiro, Brazil.

ABSTRACT

Typical schedulers of refinery crude preheat train cleaning use prediction models of the fouling factor (Rf) as a function of time or differential equations in the form of threshold models. For the former case, explicit linear and/or asymptotic models are used, not easily adaptable to flowrate and crude changes. For the latter, the rate of change of Rf is modeled as a function of the temperature and the Reynolds number, thus capturing these dependencies. However, both approaches do not capture the Reynolds number changes with deposit thickness. To address some of these shortcomings, we present a new fouling thickness growth rate model and a procedure to extract the model parameters from reconciled temperatures and flows. We also discuss how pressure drop plant data helps improve the quality of the regressions to obtain the model parameters and extensions to shell-side fouling models.

INTRODUCTION

Fouling growth has been modeled using various approaches, using empirical (linear and exponential) models and threshold models based on a certain level of transport phenomena and reaction modeling.

These models are used to make predictions of fouling as part of cleaning scheduling optimization models.

In this conference article, we focus on the proposal of a new threshold model based on fouling deposit thickness for refinery preheating trains.

REFINING CLEANING SCHEDULES

Refinery managing of heat exchanger cleaning consists of optimization models that aim at determining the cleaning schedules, that is, what exchangers to clean, at what time, and with what cleaning method (mechanical or chemical). Each of the cleaning types has a cost and a duration. The optimization is based on the fact that lack of cleaning deteriorates heat recovery and therefore increases the hot utility expenditure. However,

cleaning has a cost associated with the materials and the logistics, and at the same time, when the exchanger is taken offline to be cleaned, the heat recovery of the network lowers. To be able to make the schedule, one has to be able to:

- a) predict the fouling growth in each exchanger,
- b) determine what is the residual fouling after cleaning is performed.

Typically, a rolling horizon approach is utilized where the complete schedule is obtained for a given horizon (one to 2 years), but only the immediate cleaning recommendations are implemented. The optimization is repeated regularly, typically once a month.

Our proposed fouling thickness threshold model is an improvement over other existing models because it focuses primarily on the fouling thickness, instead of using the fouling resistance.

In the next sections, we present the thickness model, we compare it with other models. Later we discuss the use of pressure drop to improve parameter estimation and we discuss extensions of the tube side model we developed to the use of shell side threshold models.

EXISTING FOULING FACTOR MODELS

The usual form to represent the fouling impact on the behavior of a heat exchanger is to express it using a fouling resistance defined as follows:

$$Rf = \frac{1}{U} - \frac{1}{U_c} \quad (1)$$

where U is the overall heat transfer coefficient under fouled conditions and U_c is the same coefficient but under clean conditions. This equation is equivalent to the following expression for the evaluation of the overall heat transfer coefficient:

$$\frac{1}{U} = \frac{1}{hs} + \frac{dte \ln\left(\frac{dte}{dti}\right)}{2 ktube} + \frac{1}{ht} \left(\frac{dte}{dti}\right) + Rf \quad (2)$$

where ht and hs are the film coefficients of the tube-side and shell-side, respectively, dte and dti are the outer and inner tube diameter, and $ktube$ is the thermal conductivity of the tube wall.

The fouling resistance, represented in Eqs. (1) and (2) by Rf , encompass the fouling resistances in the tube-side and shell-side, Rft and Rfs :

$$Rf = Rft \left(\frac{dte}{dti} \right) + Rfs \quad (3)$$

Most research on the optimization of refinery cleaning schedules employed a classical asymptotic model to represent how the fouling resistance varies during an operational campaign [1-4]:

$$Rft = \widehat{Rft}^\infty - (\widehat{Rft}^\infty - \widehat{Rft}^0) e^{-\hat{s}t} \quad (4)$$

where \widehat{Rft}^∞ , \widehat{Rft}^0 and \hat{s} are obtained using a parameter estimation procedure from operational data.

A more comprehensive description of the fouling behavior in crude preheat trains is provided by threshold models. Ebert and Panchal developed a threshold fouling model for crude oil and other similar refinery fluids inside tubes [5]. Celebrating the 20th anniversary of the publication of the Ebert Panchal model, Wilson et al. [6] provided a very illustrative analysis of this and other models. The model is formulated as the difference between a formation rate and a removal/suppression rate:

$$\frac{dRft}{dt} = \hat{a}_1 Re^{-\hat{b}_1} e^{-\left(\frac{\hat{E}_a}{RT_{film}}\right)} - \hat{c}_1 \tau_w \quad (5)$$

where Re , T_{film} and τ_w are the Reynolds number of the fluid, the film temperature, and the shear stress at the wall. In turn, \hat{R} is the gas constant, and \hat{a}_1 , \hat{b}_1 , \hat{c}_1 , as well as \hat{E}_a , the activation energy, are parameters that were obtained using nonlinear regression of experimental data.

Several adaptations followed, as cited by Wilson et al. [6] including the insertion of the Prandtl number in the formation rate, modeling the suppression using mass transfer as well as many other considerations. Of these, there is an alternative provided by Polley et al. [7]

$$\frac{dRft}{dt} = \hat{a}_2 Re^{-\hat{b}_2} \widehat{Pr}^{-0.33} e^{-\left(\frac{\hat{E}_a}{RT_s}\right)} - \hat{c}_2 Re^{-\hat{d}_2} \quad (6)$$

This model employs the surface temperature in the formation rate instead of the film temperature and the Reynolds number in the removal/suppression rate instead of the shear stress (i.e. it represents a mass transfer effect).

We notice that the Ebert and Panchal model [5] and its adaptation by [7] were developed for fouling inside tubes. Fewer models for the shell side have been attempted [8].

The rest of this paper is to discuss conceptual problems emerging from the use of the asymptotic (Eq. (4)) and threshold models (Eqs. (5) and (6)), as it is applied to industrial practice. In particular, the targeted industrial practice we refer to is the building of fouling prediction models that can be used in the scheduling of cleaning operations in refineries.

DIFFICULTIES

The asymptotic model is mathematically simple and, for this reason, was adopted in many previous studies involving cleaning schedule optimization. However, this model has important limitations, e.g. it does not consider how the fouling rate varies with the flow rate, and as we show later, it may compromise the accuracy of the model predictions.

The threshold models have a larger extrapolation capacity because they consider the influence of the temperature and flow rate on the fouling rate. However, other drawbacks are not fully addressed in this kind of fouling model.

One of the first difficulties is that the parameters of the threshold model inside the tubes and the fouling outside the tubes on the shell side cannot be done simultaneously and must be done independently. Indeed, regressing parameters of both threshold models for both sides using experimental (plant) U values and heat transfer modeling for the heat transfer coefficients may be problematic as different sets of parameters may adjust the data well. Several papers that employed the threshold model for crude preheat trains adopted the hypothesis that the fouling in the shell-side is negligible and fouling only occurs in the tube-side (usually associated with the crude streamflow) [9-11] but, as Coletti et al. [12] pointed out, this assumption is not always true.

Another important limitation of the use of the threshold models is the fouling resistance itself. The growth of a deposited layer involves two effects:

- (i) An increasing conductive resistance, associated with the fouling layer and
- (ii) A decrease in the convective resistance is associated with the increase in the flow velocity and the consequent increase in the film transfer coefficient.

However, because the film coefficients in Eq. (2) are evaluated using the clean condition (i.e. using the inner/outer tube diameters), the fouling resistance represents both effects simultaneously. Therefore, it is interesting to observe that the term “fouling resistance” is not fully adequate to designate Rf , because it is not only associated with the conductive resistance of the fouling layer (despite this issue, we follow the literature and employ this terminology throughout our paper).

The second effect of fouling mentioned above (pressure drop) is sometimes ignored, although it may be relevant [9,13]. We show later that the

utilization of a single parameter to describe both effects (i.e. a fouling rate expressed using Rf) can limit the accuracy of the extrapolation of the model predictions. Indeed, several authors addressed the influence of the deposit layer thickness in the fouling process, considering its thermal and hydraulic impacts. However, these papers are usually based on fouling resistance rates, where the fouling thickness is evaluated accordingly [9, 12-14]. As discussed in the next section, our model does not involve fouling resistances, the fouling rate is derived from a deposit mass accumulation balance, which yields a fouling thickness growth rate model. Only a smaller number of recent papers tried to avoid the use of fouling resistance rates, similar to what is discussed here [15-16].

We concentrate on the case of fouling on the tube side only. There is some loss of generality in not considering the more complex case of fouling on both sides. However, simplicity helps clarity when concepts are presented.

HEAT TRANSFER CONSIDERING DEPOSIT THICKNESS

Instead of relying on a fouling resistance to describe the effects of the accumulation of the deposits, we propose to use the fouling thickness. Therefore, it is possible to separate more rigorously the growth of the conductive resistance due to the increase of the fouling thickness and the increase of the film coefficient due to the decrease of the free flow area. Therefore, the equivalent representation of Eq. (2) becomes [17]:

$$\frac{1}{U} = \frac{1}{hs} + \frac{dte}{2ktube} \ln\left(\frac{dte}{dti}\right) + \frac{dte}{2kft} \ln\left(\frac{dti}{dti-2\delta f_t}\right) + \frac{dte}{(dti-2\delta f_t) htf(\delta f_t)} \quad (7)$$

where kft is the thermal conductivity of the fouling layer, δf_t is the fouling layer thickness and $htf(\delta f_t)$ is the film coefficient calculated using the Reynolds number for the fouled condition; hence a function of thickness. The expression of Eq. (7) assumes a uniform fouling thickness along the heat transfer surface.

Having a model of thickness growth will help build fouling prediction models, needed for the class of scheduling models we will refer to. Before we discuss these, we discuss the proposed thickness growth models.

FOULING THICKNESS MODEL

Inspired by the Ebert and Panchal model [5,6] and the Polley et al. adaptation [7], we first propose a mass growth model for the tube side as follows:

$$\frac{dmf_t}{dt} = \alpha_t Re_t(\delta f_t)^{-n_t} Pr_t^{-r_t} e^{-\frac{E_t(c_t)}{RTs_t}} - \gamma_t Re_t(\delta f_t)^{m_t} \quad (8)$$

In the above model mf_t is the mass per unit internal tube area of the fouled layer, $E_t(c_t)$ is the activation energy for the tube side, which depends on the tube-side stream composition c_t , and TS_t is the surface temperature of the tube side. Finally, $\alpha_t, n_t, r_t, \gamma_t$ and m_t are parameters that can be obtained from plant data, similarly to how the parameters of the conventional threshold models were obtained, that is, through a regression [6].

The Reynolds number for the tube side is given by:

$$Re_t = \frac{(dti-2\delta f_t)v_t \bar{\rho} t}{\bar{\mu} t} = \frac{4 \bar{m} t}{\pi Ntp \bar{\mu} t (dti-2\delta f_t)} \quad (9)$$

where Ntp is the number of tubes per pass and $\bar{m}t$ is the tube-side flow rate.

If we assume a deposit of constant density (i.e. no aging), we can write the mass as the volume deposited times the density divided by the total area (our definition), and get:

$$mf_t = \frac{\rho f_t \pi \delta f_t (dti - \delta f_t) L Ntt}{\pi (dti - 2\delta f_t) L Ntt} = \frac{\rho f_t \delta f_t (dti - \delta f_t)}{(dti - 2\delta f_t)} \quad (10)$$

where Ntt is the total number of tubes, L is the tube length and ρf_t is the density of the tube-side deposits. Then,

$$\frac{dmf_t}{d\delta f_t} = \frac{2\rho f_t \delta f_t (dti - \delta f_t)}{(dti - 2\delta f_t)^2} + \rho f_t \quad (11)$$

Therefore, we arrive at:

$$\frac{d\delta f_t}{dt} = \frac{(dti - 2\delta f_t)^2}{2\rho f_t \delta f_t (dti - \delta f_t) + (dti - 2\delta f_t)^2 \rho f_t} \left(\alpha_t Re_t(\delta f_t)^{-n_t} Pr_t^{-r_t} e^{-\frac{E_t(c_t)}{RTb_t}} - \gamma_t Re_t(\delta f_t)^{m_t} \right) \quad (12)$$

Thus, by modeling the thickness growth, one is capable of better assessing the effects of fouling.

It is possible to integrate Eq. (12) using a model of the heat exchanger and therefore evaluate the variation of the fouling thickness during the operational period of the heat exchanger. Using Eq. (2) and Eq. (7) it is possible to express the result of fouling thickness in terms of the fouling resistance (Lemos et al., 2022):

$$Rft = \frac{dti}{2kft} \ln\left(\frac{dti}{dti-2\delta f_t}\right) + \frac{dti}{dti-2\delta f_t} \frac{1}{htf(\delta f_t)} - \frac{1}{ht} \quad (12)$$

This allows an easier comparison with the other models.

MODEL COMPARISON

We consider real data from a heat exchanger operating in a refinery. The investigated period corresponds to about four months. The hot stream is jet-fuel and the cold stream is crude oil. The problem parameters are presented in Table 1. We point out that these data correspond to varying flowrate, as shown in Figure 1. The deposit thermal conductivity was assumed to be equal to 0.2 W/(m·K), a typical value of a fresh deposit [16].

We applied a parameter estimation methodology to the operational data of this heat exchanger to obtain the parameters of the thickness model as well as the Polley model and the asymptotic model. The parameters were estimated considering the data of the first half of the investigated period (“training set”), and the remaining data were used to assess the accuracy of the models (“test set”).

Table 1. Heat exchanger parameters.

Parameter	Value
D_s (m)	0.94
d_{te} (m)	0.03819
N_{tt}	240
N_{tp}	120
rp	1.875
Layout (°)	90
L (m)	5.7912
Number of baffles	16
Baffle cut (%)	19
Tube thickness (m)	0.002769

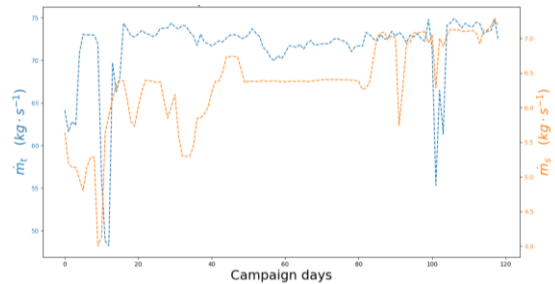


Fig. 1: Flowrate profiles

Figure 2 shows the Rf values obtained through a reconciliation procedure and the simulation results. Figure 3 shows the corresponding heat load of the crude stream. Table 2 displays the deviations for each model in the test set. The estimated parameters are shown in Table 3.

Figures 2, 3, and Table 2 show that the asymptotic model exhibits the worst performance. The gap is particularly high at the end of the investigated period. Table 3 shows the results for the estimated parameters. Table 4 shows the parameters corresponding to the asymptotic model.

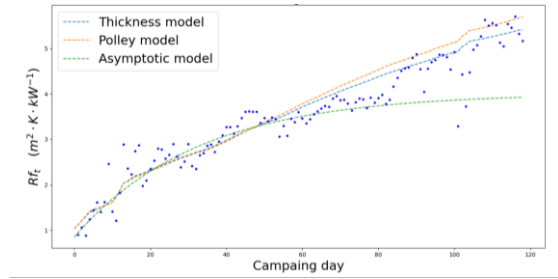


Fig. 2: Fouling data and models output

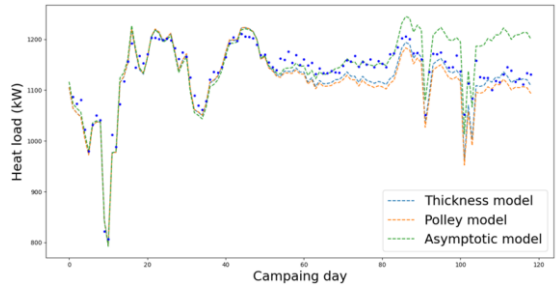


Fig. 3: Profiles of the heat load of the crude stream

Table 2. Deviations between the operational data and the models' output

Deviation (%)	Polley model	Thickness model	Asymptotic model
Test	10.31	7.58	13.54

Table 3. Parameters of the Polley and the Thickness models

	Polley model	Thickness model
E_t (kJ/mol)	30.5	20.0
α_t ($K^1m^2W^{-1}day^{-1}$)	$1.27 \cdot 10^4$	$1.19 \cdot 10^5$
γ_t ($K^1m^2W^{-1}day^{-1}$)	$1.46 \cdot 10^{-8}$	$2.45 \cdot 10^{-6}$

Table 4. Parameters of the asymptotic model

	Asymptotic model
\widehat{Rf}_t^∞ ($K^1m^2W^{-1}$)	$4.01 \cdot 10^{-3}$
\widehat{Rf}_t^0 ($K^1m^2W^{-1}$)	$8.50 \cdot 10^{-4}$
s (day^{-1})	0.0306

The fouling resistance predictions of the thickness model present the best adherence to the operational data in the test set. The output of the Polley and thickness models are similar during the training period, but an increasing gap is observed in the test period.

The increasing gap between the thickness and Polley models occurs due to the increase of the fouling thickness predicted by the thickness model,

as illustrated in Figure 4 (the Polley model ignores the variation of the Re due to the higher velocity resultant from the deposits). The increase of the fouling thickness brings a modification of the Reynolds number, which decreases the fouling rate. Figure 5 shows the crescent gap between the Reynolds number due to the thickness increase.

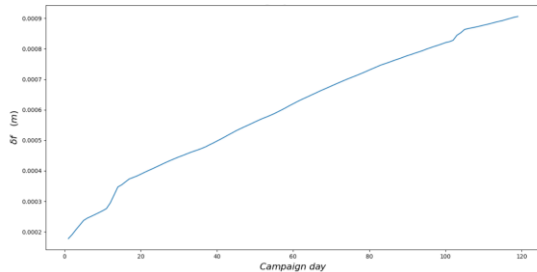


Fig. 4: Fouling thickness profile

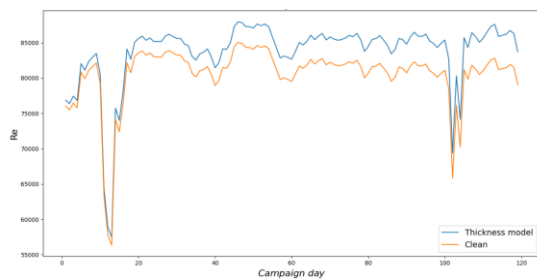


Fig. 5: Comparison of the Reynolds number profiles between the thickness and Polley models

Next, a simulation using the above-regressed parameters was performed using the three models during an extrapolation period of four additional months. The comparison of the Rf profiles for the total eight months period is shown in Figure 6. During the extrapolation period, the simulation was conducted using a constant flowrate.

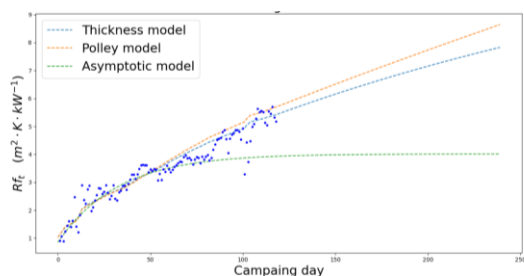


Fig. 6: Fouling data and model output including an extrapolation period

According to Figure 6, the asymptotic model predicts an almost constant fouling resistance during the extrapolation period, but the threshold models indicate a continuous increase. This difference shows the limitation of the asymptotic model to represent the behavior of threshold models.

The output of the threshold models in Figure 6 presents an increasing difference in the

extrapolation period. The Polley model overpredicts the fouling resistance because it dismisses the increase of the Reynolds number due to the reduction of the free flow area. The heat load predicted by the Polley model is 3.6% lower than the thickness model evaluation at the end of the period.

The above results show that the asymptotic model needs to be abandoned. Next, the Polley model, which ignores thickness renders sizable differences in the heat transfer. Indeed, a 3.6% difference compounded over different exchangers in a schedule introduces sizable differences in cleaning scheduler results.

USE OF PRESSURE DROP MODELING

Models to obtain the pressure drop in fouled tubes are available [13]. In the case of parameter estimation of the fouling model (Eq. (11)), one can also add the equation of pressure drop as a function of the Reynolds number, now calculated based on the thickness of the deposits. Thus, when estimating parameters, where the square of the relative deviation of calculated U values from experimental U values, or the equivalent Rf values, is minimized, one can add the square of the relative difference between a predicted pressure drop and the measured one. This adds redundancy to the system. Arguably, the pressure drop is not always measured for individual exchangers, but for many in series, so the solution may be to perform parameter estimation for all these exchangers simultaneously. This issue is not explored further in this conference article.

VALUE OF THICKNESS MODELING

Aside from the above-discussed advantages of thickness modeling, namely, the improved fouling prediction capacities, which improves the performance of the cleaning scheduler, there are other advantages:

- When the thickness of deposits can be predicted, the increase in pumping costs is also predictable, something that is not properly available with current threshold models. The addition of this cost to the cost of fouling (furnace load increase) might change the trade-off between cleaning benefits and costs in optimal cleaning schedules.
- Knowing and/or being capable of predicting the thickness profile through time, also allows for determining the deposit age profile. Indeed, it is known that deposits pass through different transformations (chemical reactions) through time ending in inner layers with diffuse boundaries that are called coke. Thus, the profile of density, as well as the hardness of the deposits, can be somehow anticipated. Because the inner hard layers are difficult to remove, cleaning efficiency varies with age. This is true for mechanical cleaning methods such as hydro blasting or ultrasonic methods, but it is also particularly important in the case of chemical

cleaning methods, where the inner aged layers are harder to remove if at all.

- Therefore, age prediction helps the cleaning schedule optimization because a new trade-off is included, one that ponders the economic advantage of selecting the right cleaning method, aside, of course, from the improvement in the accuracy of the optimization.

SHELL SIDE FOULING MODEL

Some authors have argued that fouling on the shell side rarely takes place [11], or that they obey a simple law of steady (albeit slow) linear growth [18]. It is possible to speculate that exchangers in preheating trains of topping units that handle products (Kero, Diesel, Jet Fuel, and even AGO) do not have fouling precursors because they would have to travel in vapor form in the rectifying section of these columns. Because of these speculations, fouling on the shell side (the usual allocation of these streams) is usually considered negligible, or very slow. However, the topped crude is usually allocated either on the tube or the shell side of exchangers in the preheating train and it has an even larger concentration of fouling deposit precursors. Because they are paired with raw crude on the other side, the modeling of the fouling growth on the shell side is inevitable [8].

Fouling in the shell-side also inserts an additional conductive resistance associated with the fouling layer over the thermal surface. A fluid dynamic effect represented by the increase of the flow resistance due to the reduction of the free flow area also takes place. This is more a complex phenomenon than the one taking place inside tubes. Indeed, it is associated with the reduction of the free flow area along the different clearances (tube-baffle, baffle-shell, and bundle-shell), which modifies the flow distribution among the leakage and by-pass streams, thus leading to different flow patterns and, consequently, fouling rates.

For fouling on the shell side, one can develop an equation that is similar to Eq. (11) if one assumes that fouling also takes place on the outside of the tubes, provided that the right Reynolds number is used. One can (over) simplify the model to consider, for example, a Reynolds number corresponding to flow perpendicular to the bank of tubes. A more complex model would need to discuss deposits taking place when the flow is parallel to the tubes and also different fouling rates associated with the clearances.

As stated above, it would be rare to find exchangers handling topped crude (residue) that do not foul on the raw crude side. Thus, even though thickness threshold models can be developed for different regions of the shell side, the parameter estimation of both models (tube and shell side) needs to take place. Considering that the only thing experimentally available is the U value and the

pressure drops (assuming they are used), the uniqueness of the set of parameters obtained is in question, especially if one can show that there possibly exist multiple solutions. While pressure drop is of great help, it may not be enough. Possibly, validation of these models using field data may require measuring the thickness of the deposits when the exchangers are opened for cleaning, adding thus a parameter in the form of “final thickness”. We leave this work for future research.

CONCLUSION

In this article, we proposed a thickness-based threshold model for the determination of the fouling growth rate and show the advantages of this model as compared to the use of asymptotic models and one existing threshold model that does not consider deposit thickness. Finally, we discussed the addition of pressure drop considerations in the parameter estimation of the thickness threshold model and its usefulness for predicting cleaning effectiveness based on aging. We also discussed extensions to shell-side fouling models.

NOMENCLATURE

d_{te}	Outer tube diameter, m
d_{ti}	Inner tube diameter, m
h_s	Film coefficients of the shell-side, W/m ² K
h_t	Film coefficients of the tube-side, W/m ² K
h_f	Film coefficient calculated using the Reynolds number for the fouled condition, W/m ² K
k_{tube}	Thermal conductivity of the tube wall, m K/W
L	Tube length, m
n_t	Thickness model parameter, dimensionless
N_{tp}	Number of tubes per pass, dimensionless
N_{tt}	Total number of tubes, dimensionless
Nu	Nusselt number, dimensionless
m_{f_t}	Mass per unit internal tube area of the fouled layer, kg/m ²
m_t	Thickness model parameter, dimensionless
\widehat{m}_t	Tube side mass flow rate, kg/s
R	Gas constant, J/mol K
r_t	Thickness model parameter, dimensionless
Re	Reynolds number, dimensionless
R_f	Fouling resistance, m ² K/W
R_{fs}	Fouling resistances in the shell-side, m ² K/W
R_{ft}	Fouling resistances in the tube-side, m ² K/W
$\widehat{R}_{f_t}^{\infty}$	Asymptotic model parameter, m ² K/W
$\widehat{R}_{f_t}^0$	Asymptotic model parameter, m ² K/W
\hat{s}	Asymptotic model parameter, 1/day
T	Temperature, K
T_{s_t}	Surface temperature of the tube side, K
T_{film}	Film temperature, K
U	overall heat transfer coefficient under fouled conditions W/m ² K
U_c	overall heat transfer coefficient under clean conditions W/m ² K
v_t	Tube side velocity
σ	Stefan-Boltzmann constant, kW/m ² K ⁴

\hat{a}_1 Ebert and Panchal model parameter, $m^2 kW^{-1} h^{-1}$
 \hat{b}_1 Ebert and Panchal model parameter, dimensionless
 \hat{c}_1 Ebert and Panchal model parameter, $m^2 kW^{-1} h^{-1} Pa^{-1}$
 \hat{a}_2 Polley model parameter, $m^2 kW^{-1} h^{-1}$
 \hat{b}_2 Polley model parameter, dimensionless
 \hat{c}_2 Polley model parameter, $m^2 kW^{-1} h^{-1}$
 \hat{d}_2 Polley model parameter, dimensionless
 \hat{E}_a Activation energy, J/mol
 τ_w Shear stress, Pa
 δf_t Fouling layer thickness, m
 α_t Thickness model parameter, $m^2 K W^{-1} day^{-1}$
 γ_t Thickness model parameter, $m^2 K W^{-1} day^{-1}$
 $\hat{\mu}_t$ Tube side viscosity, Pa s
 $\hat{\rho}_t$ Tube side density kg/m³
 ρf_t Density of the tube-side deposits, kg/m³

Subscript

Subscripts and superscripts should be identified under a separate second-level heading.

i inner
o outer
w wall

REFERENCES

- [1] Smaili, F., Vassiliadis, V. S., Wilson, D. I., Mitigation of Fouling in Refinery Heat Exchanger Networks by Optimal Management of Cleaning, *Energy & Fuels* 2001, 15, 1038-1056.
- [2] Lavaja, J. H., Bagajewicz, M. J., On a New MILP Model for the Planning of Heat-Exchanger Network Cleaning. Part II: Throughput Loss Considerations, *Ind. Eng. Chem. Res.* 2005, 44, 8046-8056.
- [3] Ismaili, R. A., Lee, M. W., Wilson, D. I., Vassiliadis, V. S., Heat exchanger network cleaning scheduling: From optimal control to mixed-Integer decision making, *Computers and Chemical Engineering* 111 (2018) 1–15.
- [4] Ismaili, R. A., Lee, M. W., Wilson, D. I., Vassiliadis, V. S., Optimisation of heat exchanger network cleaning schedules: Incorporating uncertainty in fouling and cleaning model parameters, *Computers and Chemical Engineering* 121 (2019) 409–421
- [5] Ebert, W. and Panchal, C.B., in *Fouling Mitigation of Industrial Heat Exchange Equipment*, eds. Panchal, C.B., Bott, T.R., Somerscales, E.F.C. and Toyama, S., pp. 451-460, Begell House, NY, 1997.
- [6] Wilson, D. I., Ishiyama E. M., Polley, G. T. *Heat Transfer Engineering*. Vol. 38, 2017- Issue 7-8. Selected papers presented at the heat exchanger fouling and cleaning conference, Jun2 7-12, 2015. Enfield (Dublin), Ireland.
- [7] Polley, G.T., Wilson, D.I., Yeap, B.L. and Pugh, S.J., *Use of crude oil threshold data in heat exchanger design*, *Applied Thermal Engineering* (2002), 22, 763-776.
- [8] Bejarano, E.D., Coletti, F., Macchietto, S., Modeling and Prediction of Shell-Side Fouling in Shell-and-Tube Heat Exchangers, *Heat Transfer Engineering* 2019, vol. 40, n°. 11, 845–861
- [9] Ishiyama, E.M., Paterson, W.R., Wilson, D.I., Platform for Techno-economic Analysis of Fouling Mitigation Options in Refinery Preheat Trains., *Energy & Fuels* 2009, 23, 1323–1337
- [10] Ishiyama, E.M., Heins, A.V., Paterson, W.R., Spinelli, L., Wilson, D.I., Scheduling cleaning in a crude oil preheat train subject to fouling: Incorporating desalter control., *Applied Thermal Engineering* 30 (2010) 1852-1862.
- [11] Bejarano, E.D., Santos, M.Y., Dopico, M.G., Fuentes, L.L., Coletti, F., The Impact Of Fouling On The Optimal Design of A Heat Exchanger Network: An Industrial Case Study., *Heat Exchanger Fouling and Cleaning – 2017*.
- [12] Coletti, F., Macchietto, S., A Dynamic, Distributed Model of Shell-and-Tube Heat Exchangers Undergoing Crude Oil Fouling., *Ind. Eng. Chem. Res.* 2011, 50, 4515–4533.
- [13] Yeap, B.L., Wilson, D.I., Polley, G.T., Pugh, S.J., Mitigation of Crude Oil Refinery Heat Exchanger Fouling Through Retrofits Based on Thermo-Hydraulic Fouling Models., *Chemical Engineering Research and Design*. 2004, 82(A1): 53-71.
- [14] Ishiyama, E.M., Paterson, W.R., Wilson, D.I., Thermo-hydraulic channelling in parallel heat exchangers subject to fouling., *Chemical Engineering Science*. 2008, 63, 3400-3410.
- [15] Bejarano, E.D., Coletti, F., Macchietto, S. A New Dynamic Model of Crude Oil Fouling Deposits and Its Application to the Simulation of Fouling-Cleaning Cycles., *AIChE Journal*. 2016, 62, 90–107.
- [16] Bejarano, E.D., Coletti, F., Macchietto, S., A Model-Based Method for Visualization, Monitoring, and Diagnosis of Fouling in Heat Exchangers., *Ind. Eng. Chem. Res.* 2020, 59, 4602-4619.
- [17] Lemos, J.C., Costa, A.L.H., Bagajewicz, M.J., Design of shell and tube heat exchangers considering the interaction of fouling and hydraulics., *AIChE Journal*. <https://aiche.onlinelibrary.wiley.com/doi/abs/10.1002/aic.17586>
- [18] Fuentes, J.L., Jobson, M., Smith, R., Estimation of Fouling Model Parameters for Shell Side and Tube Side of Crude Oil Heat Exchangers Using Data Reconciliation and Parameter Estimation., *Ind. Eng. Chem. Res.* 2019, 58, 10418–10436.